Title

Whole DNA methylome profiling in mice exposed to secondhand smoke

Journal

Epigenetics, 7(11)

ISSN

1559-2294

Authors

Tommasi, Stella

Zheng, Albert

Yoon, Jae-In

et al.

Publication Date

2012-11-13

DOI

10.4161/epi.22453

Peer reviewed

RESEARCH PAPER

Epigenetics 7:11, 1–13; November 2012; © 2012 Landes Bioscience

Whole DNA methylome profiling in mice exposed to secondhand smoke

Stella Tommasi,[1] Albert Zheng,[1] Jae-In Yoon,[1] Arthur Xuejun Li,[2] Xiwei Wu[2] and Ahmad Besaratinia[1,*]

[1]Department of Cancer Biology; Beckman Research Institute of the City of Hope; Duarte, CA USA; [2]Department of Molecular Medicine; Beckman Research Institute of the City of Hope; Duarte, CA USA

Keywords: DNA methylation, epigenetics, lung cancer, nonsmokers, repetitive DNA elements

Aberration of DNA methylation is a prime epigenetic mechanism of carcinogenesis. Aberrant DNA methylation occurs frequently in lung cancer, with exposure to secondhand smoke (SHS) being an established risk factor. The causal role of SHS in the genesis of lung cancer, however, remains elusive. To investigate whether SHS can cause aberrant DNA methylation in vivo, we have constructed the whole DNA methylome in mice exposed to SHS for a duration of 4 mo, both after the termination of exposure and at ensuing intervals post-exposure (up to 10 mo). Our genome-wide and gene-specific profiling of DNA methylation in the lung of SHS-exposed mice revealed that all groups of SHS-exposed mice and controls share a similar pattern of DNA methylation. Furthermore, the methylation status of major repetitive DNA elements, including long-interspersed nuclear elements (LINE L1), intracisternal A particle long-terminal repeat retrotransposons (IAP-LTR), and short-interspersed nuclear elements (SINE B1), in the lung of all groups of SHS-exposed mice and controls remains comparable. The absence of locus-specific gain of DNA methylation and global loss of DNA methylation in the lung of SHS-exposed mice within a timeframe that precedes neoplastic-lesion formation underscore the challenges of lung cancer biomarker development. Identifying the initiating events that cause aberrant DNA methylation in lung carcinogenesis may help improve future strategies for prevention, early detection and treatment of this highly lethal disease.

Introduction

In the past few decades, a large body of epidemiologic evidence has accumulated that links secondhand smoke (SHS) exposure to lung cancer in nonsmokers.[1-4] Yet, the underlying mechanism of SHS carcinogenicity in nonsmokers' lung cancer remains unknown.[5] Understanding the mechanism of action of SHS in the genesis of lung cancer in nonsmokers is important because (1) there is a global burden of SHS imposed by 1.2 billion smokers[3,6] and (2) lung cancer continues to take its toll as the leading cause of cancer-related mortalities worldwide.[7,8] As a research priority, therefore, it is imperative to determine the mechanistic involvement of SHS in the development of human lung cancer.[5] Elucidating the mechanistic role of SHS in the pathogenesis of lung cancer can help decipher many aspects of this disease, which can potentially be exploited for preventive, therapeutic and prognostic purposes.[9,10]

Aberration of DNA methylation is the best-studied epigenetic mechanism of carcinogenesis.[11-14] Aberrant DNA methylation in cancer manifests as global loss of DNA methylation (hypomethylation) and/or locus-specific gain of DNA methylation (hypermethylation).[11,13,15] Whereas DNA hypomethylation is thought to contribute to oncogenesis by reactivation of latent retrotransposons, induction of genomic instability, and activation of proto-oncogenes,[16,17] DNA hypermethylation is believed to elicit tumorigenesis by dysregulation of gene expression, e.g., through transcriptional silencing of tumor suppressor genes.[15,18,19] In mammalian genomes, aberrant DNA methylation occurs almost exclusively in the context of 5'-CpG-3' dinucleotides (CpGs).[11,20] Hypermethylation of high-density CpG regions, termed CpG islands,[21] clustered at the promoter, untranslated 5'-region and exon 1 of known genes (promoter CpG islands) or localized within gene bodies (intragenic CpG islands) is a common event in carcinogenesis.[12-14,19] Global DNA hypomethylation at repetitive DNA elements, such as long- and short-interspersed nuclear elements (LINE and SINE, respectively) and long-terminal repeat retrotransposons (LTR) is also a frequent occurrence in cancer.[17,22,23]

Recently, we have demonstrated a genotoxic mode of action for SHS based on the ability of this carcinogen to induce DNA adduct-driven mutagenesis in transgenic Big Blue® mice.[24,25] In the present study, we have expanded this investigation to determine whether SHS can also cause epigenetic effects through aberration of DNA methylation. Here, for the first time, we have globally profiled DNA methylation in the lung of mice exposed to SHS for a duration of 4 mo, both after the termination of exposure and at ensuing intervals post-exposure (up to 10 mo). We have used a genome-wide microarray-based approach[26,27] to catalog the DNA methylation profile in the lung of SHS-exposed mice before and after various recovery periods. For verification

*Correspondence to: Ahmad Besaratinia; Email: abesaratinia@gmail.com
Submitted: 08/02/12; Revised: 09/19/12; Accepted: 10/04/12
http://dx.doi.org/10.4161/epi.22453

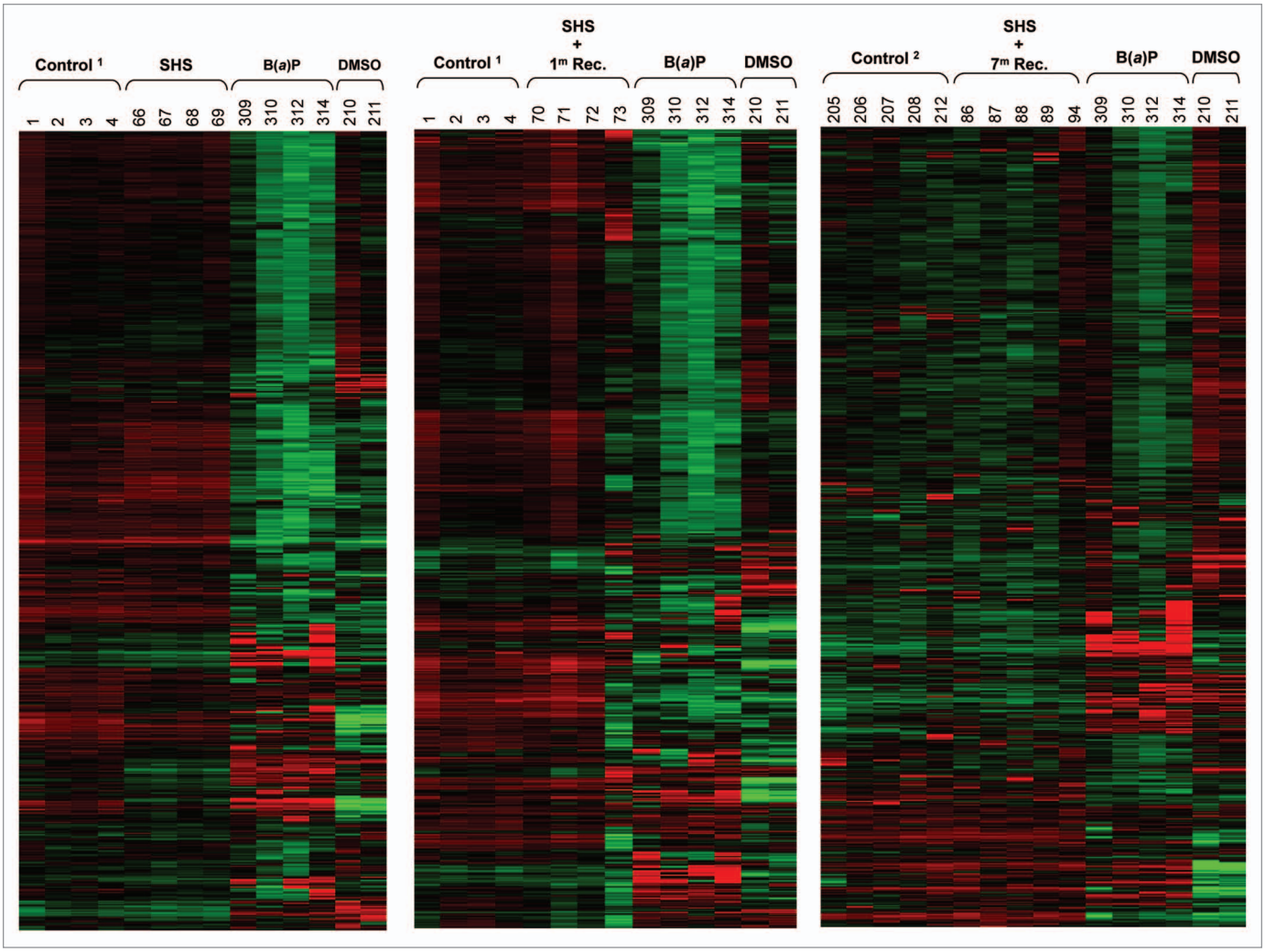

Figure 1. Genome-wide profiling of DNA methylation in SHS-exposed mice vs. control. The Hierarchical Clustering Analysis was used to generate heatmaps of DNA methylation profile in the lung of SHS-exposed mice and control. Representative heatmaps from samples of SHS-exposed mice (immediately after treatment, and after 1 mo and 7 mo recovery periods) and control are shown. Of note, the three panels show three different sets of several thousand CpG islands representing three snap shots of the whole methylome. To account for "age" as a potential confounder, two groups of control mice, including control[1] (6 mo old clean-air mock-treated mice) and control[2] (16 mo old clean-air mock-treated mice) were used. Numbers indicate mouse IDs. For comparison, heatmaps of DNA methylation profile in tumor DNA from B(*a*)P-treated mice vs. control (DMSO) are shown.

purposes, we have confirmed the data obtained by our microarray-based analysis using the conventional combined bisulfite-restriction analysis (COBRA),[28] and sodium bisulfite genomic sequencing.[29] Furthermore, we have determined the methylation status of major repetitive DNA elements, including LINE L1, intracisternal A particle (IAP) LTR and SINE B1,[30-32] in the lung of SHS-exposed mice, both before and after the recovery periods, using a bisulfite-based sequencing analysis.[33]

Results

We have used the methylated-CpG island recovery assay (MIRA) in combination with microarray analysis[26,27] to detect changes in DNA methylation, genome-wide, in the lung of mice exposed to SHS for a duration of 4 mo, immediately after the termination of exposure and at various recovery times, e.g., 1, 4, 7 and 10 mo after SHS-exposure. Genomic DNA was isolated from the lung of SHS-exposed and control mice, and enriched for methylated CpG islands by the MIRA pull-down procedure.[26,27] Subsequently, the enriched- and input-DNA fractions were labeled, mixed, and hybridized to the mouse CpG island plus promoter tiling arrays (Roche NimbleGen Inc.). The microarray data were analyzed using a stringent bioinformatics approach with algorithms for peak calling, as described in Materials and Methods. Using this approach, we found a similar pattern of DNA methylation in the lung of SHS-exposed mice and control, both before and after various recovery periods. The resemblance of DNA methylation profile in the lung of SHS-exposed mice and control is shown in **Figure 1**, which is an assembly of DNA methylation heatmaps from representative samples of SHS-exposed mice and control, immediately after treatment and 1 and 7 mo post-treatment. The heatmaps were

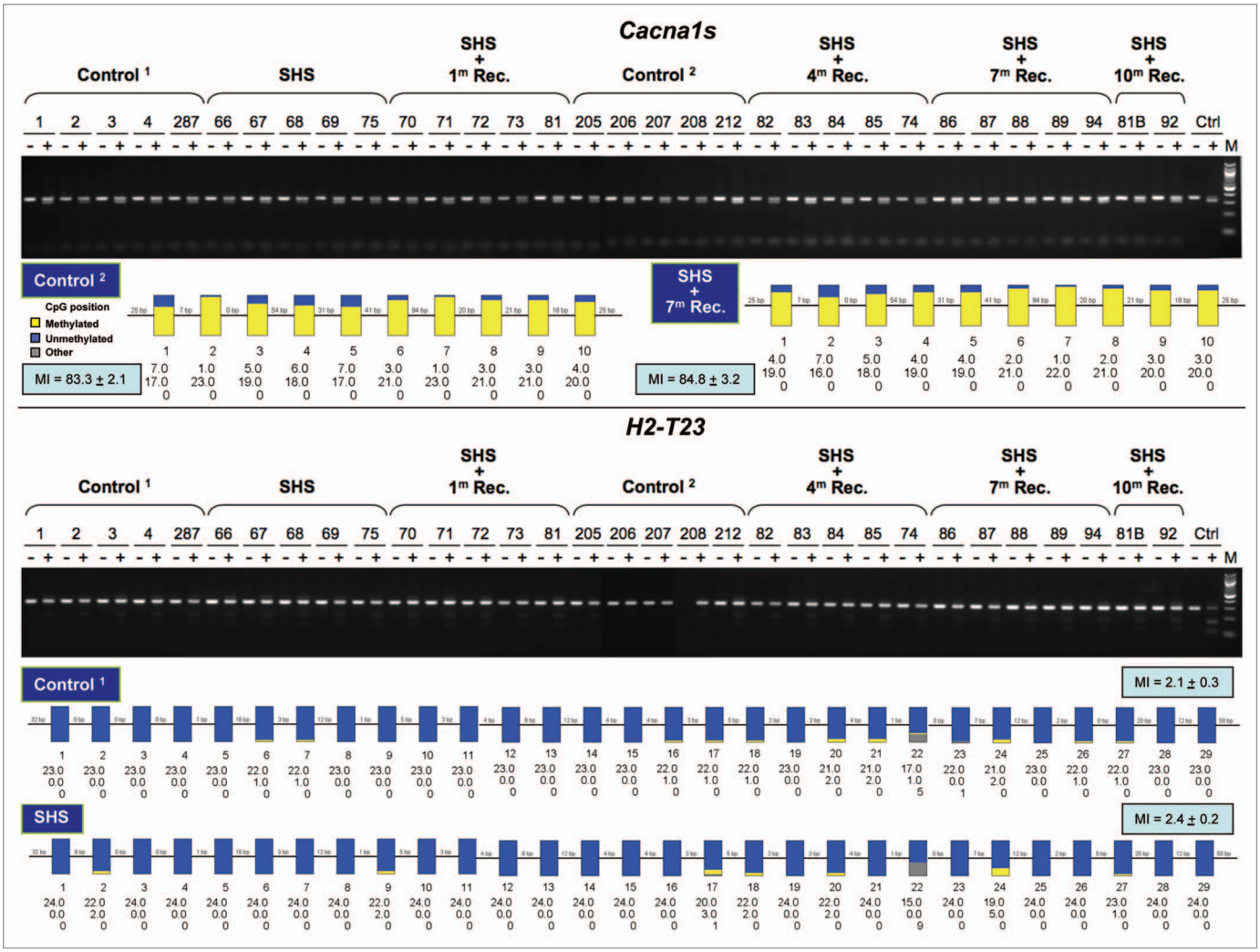

Figure 2. Verification of marginal hypermethylation in the *Cacna1* gene and hypomethylation in the *H2-T23* gene in SHS-exposed mice vs. control. Genomic DNA isolated from the lung of SHS-exposed and control mice was treated with sodium bisulfite, and the CpG islands within the *Cacna1s* and *H2-T23* genes were amplified with gene-specific primers, and subjected to COBRA.[28] Representative results for samples of SHS-exposed mice (before and after 1, 4, 7 and 10 mo recovery periods) and control are shown (upper panels). The COBRA results consistently show no differences in the extent of DNA methylation in the specified CpG islands between experimental and control mice. Digested fragments on the gel are indicative of methylated *BstUI* restriction sites (5'-CG▲CG) within the *Cacna1s* CpG island, and TaqI restriction sites (5'-T▲CGA) within the *H2-T23* CpG island. Mouse genomic DNA, isolated from the lung, was methylated in vitro with the SssI methyltransferase, and served as control (Ctrl). (+) and (-) represent the presence and absence, respectively, of the restriction enzymes in the reaction mix. Numbers indicate mouse IDs. M, 100 bp ladder DNA marker. The extent of CpG methylation within the *Cacna1s* and *H2-T23* CpG islands was determined by sodium-bisulfite sequencing[29] in the lung genomic DNA from SHS-exposed and control mice. Based on microarray data, samples of SHS-exposed mice, which showed the highest hyper/hypomethylation in the specified CpG islands, were subjected to bisulfite genomic sequencing (lower panels). The sequencing results of randomly selected independent clones from both the experimental and control mice were analyzed using the BIQ Analyzer software (http://biq-analyzer.bioinf.mpi-inf.mpg.de/). The methylation status of each individual CpG dinucleotide within the *Cacna1s* and *H2-T23* CpG islands per experimental and control groups is indicated by the number of methylated-, unmethylated, and mutated (other) CpGs detected in the sequenced clones from each group of experimental or control mice. The heights of yellow, blue, and gray bars, respectively, represent the percentages of methylated, unmethylated, and mutated CpGs at each CpG dinucleotide within the *Cacna1s* and *H2-T23* CpG islands. Numbers along the reference sequence show the distance between interrogated CpGs within the *Cacna1s* and *H2-T23* CpG islands. Average results per experimental or control groups are shown as Methylation Index (MI = mean ± SD). Marginal differences in MI between experimental and control mice were not statistically significant (Fisher's exact test).

generated by the Complete-Linkage Hierarchical Clustering, which uses the Pearson's Dissimilarity to measure differences between DNA methylation profiles among different samples. As shown in **Figure 1**, all samples from SHS-exposed mice and control, both before and after the recovery periods, clustered very closely together. Using the stringent bioinformatics criteria as described in Materials and Methods, we found no hyper- or hypo-methylated targets that were commonly present across all samples of any group of SHS-exposed mice relative to control. For comparison purposes, we have performed the MIRA-microarray analysis on tumor DNA from mice treated intraperitoneally (i.p.) with benzo(*a*)pyrene [B(*a*)P], a

Table 1. Differentially methylated targets detected in the lung DNA of SHS-exposed mice *versus* controls

Gene symbol	Description	Ratio (log2)	Peak location	Relative to gene	Hyper-/Hypo-methylation	Comparison groups
H2-T23	Histocompatibility 2, T region locus 23	1.31	Chr 17: 36168923-36169462	Upstream/Intragenic	Hypo	SHS *vs* Ctrl[1]
H2-T23	Histocompatibility 2, T region locus 23	1.25	Chr 17: 36168923-36169462	Upstream/Intragenic	Hypo	SHS [(1m Rec.)] *vs* Ctrl[1]
Olfr48	Olfactory receptor 48	1.19	Chr 2: 89684713-89685070	Upstream/Intragenic	Hyper	SHS [(1m Rec.)] *vs* Ctrl[1]
Fktn	Fukutin	2.08	Chr 4: 53726988-53727528	Upstream	Hyper	SHS [(1m Rec.)] *vs* Ctrl[1]
Unknown	-	1.03	Chr 15: 98210800-98211049	-	Hypo	SHS [(7m Rec.)] *vs* Ctrl[2]
Cacna1s	Calcium channel, voltage-dependent, L type, alpha 1S subunit	1.05	Chr 1: 137949472-137949926	Upstream	Hyper	SHS [(7m Rec.)] *vs* Ctrl[2]
Bdkrb1	Bradykinin receptor, beta 1	1.38	Chr 12: 106842483-106843037	Upstream/Intragenic	Hyper	SHS [(7m Rec.)] *vs* Ctrl[2]
Gja8	Gap junction protein, alpha 8	1.35	Chr 3: 96729615-96730184	Upstream	Hyper	SHS [(7m Rec.)] *vs* Ctrl[2]

To account for age-associated variability, two groups of control mice, including control[1] (ctrl[1], 6 month-old clean-air mock-treated mice) and control[2] (ctrl[2], 16 month-old clean-air mock-treated mice) were used.

prominent constituent of SHS[5,34] and a potent multi-organ carcinogen.[35,36] As shown in **Figure 1**, the profile of DNA methylation in tumor DNA from B(*a*)P-treated mice was significantly different from that in control, as reflected in the distinct heatmaps generated for the respective samples. We found 251 hypermethylated targets and 121 hypomethylated targets that were commonly present across all the B(*a*)P-induced tumors relative to control. We note that control mice were treated with solvent dimethyl sulfoxide (DMSO) using the same protocol as used for B(*a*)P treatment. As tumors in B(*a*)P-treated mice originated from the accessory sex organs, we took control samples from the same anatomical site in DMSO-treated mice (Tommasi et al., ongoing project).

Next, we used more relaxed bioinformatics criteria for the detection of aberrantly methylated targets in samples of SHS-exposed mice, i.e., a methylation peak being present in all but one sample from each group of experimental mice relative to control. The rationale behind using these less strict criteria was to find target genes that were differentially methylated in a majority but not all the SHS-exposed mice. Obviously, such potentially important target genes would go undetected if the stringent criteria (i.e., methylation peaks being present in all SHS-exposed mice) were used in the analysis. Applying the more relaxed criteria, we found 1–3 marginally hypermethylated or hypomethylated targets within a few groups of SHS-exposed mice relative to control. **Table 1** summarizes relevant information on the differentially methylated target genes detected in the lung of SHS-exposed mice vs. control. The identified methylated or demethylated targets in the lung of SHS-exposed mice were, however, deemed non-significant as the validation analysis by the COBRA and bisulfite sequencing[28,29] showed no appreciable differences in the extent of DNA methylation in these targets between experimental and control mice (see below).

As mentioned above, we have also validated the MIRA-microarray data by randomly selecting several targets that were identified as marginally hyper- or hypo- methylated in a few groups of SHS-exposed mice relative to control, and analyzed them by the conventional COBRA and bisulfite sequencing.[28,29] In all cases, we verified the data obtained by the MIRA-microarray analysis as we confirmed that there were no statistically significant differences in the extent of DNA methylation in any of the analyzed targets between SHS-exposed mice and control. **Figure 2** shows representative results of the COBRA and bisulfite sequencing for the marginally methylated target *Cacna1s*, and demethylated target *H2-T23* identified by the MIRA-microarray analysis. Detailed bisulfite sequencing results showing the methylation status of individual CpGs within the *Cacna1s* and *H2-T23* CpG islands in each mouse in both experimental and control groups are also provided in **Figures S1 and S2**, respectively. As shown, both the COBRA and bisulfite sequencing analyses verified that there were no statistically significant changes in the extent of DNA methylation in any of the above-specified targets between experimental and control mice (Fisher's exact test).

Figure 3 (See opposite page). Methylation profiling of LINE L1 repetitive DNA elements in SHS-exposed mice vs. control. Bisulfite sequencing of LINE L1 elements was performed on genomic DNA isolated from the lung of SHS-exposed and control mice using a published protocol.[33] Representative results for samples of SHS-exposed mice (immediately after treatment, and after 1, 4, 7 and 10 mo recovery periods) and control are shown. The methylation status of each individual CpG dinucleotide within the LINE L1 element per experimental and control groups is indicated by the number of methylated, unmethylated and mutated (other) CpGs detected in the sequenced clones from each group of experimental or control mice. The heights of yellow, blue and gray bars, respectively, represent the percentages of methylated-, unmethylated-, and mutated-CpGs at each CpG dinucleotide within the LINE L1 element. Numbers along the reference sequence show the distance between interrogated CpGs within the LINE L1 element. Average results per experimental or control groups are shown as Methylation Index (MI = mean ± SD). Marginal differences in MI between experimental and control mice were not statistically significant (Fisher's exact test).

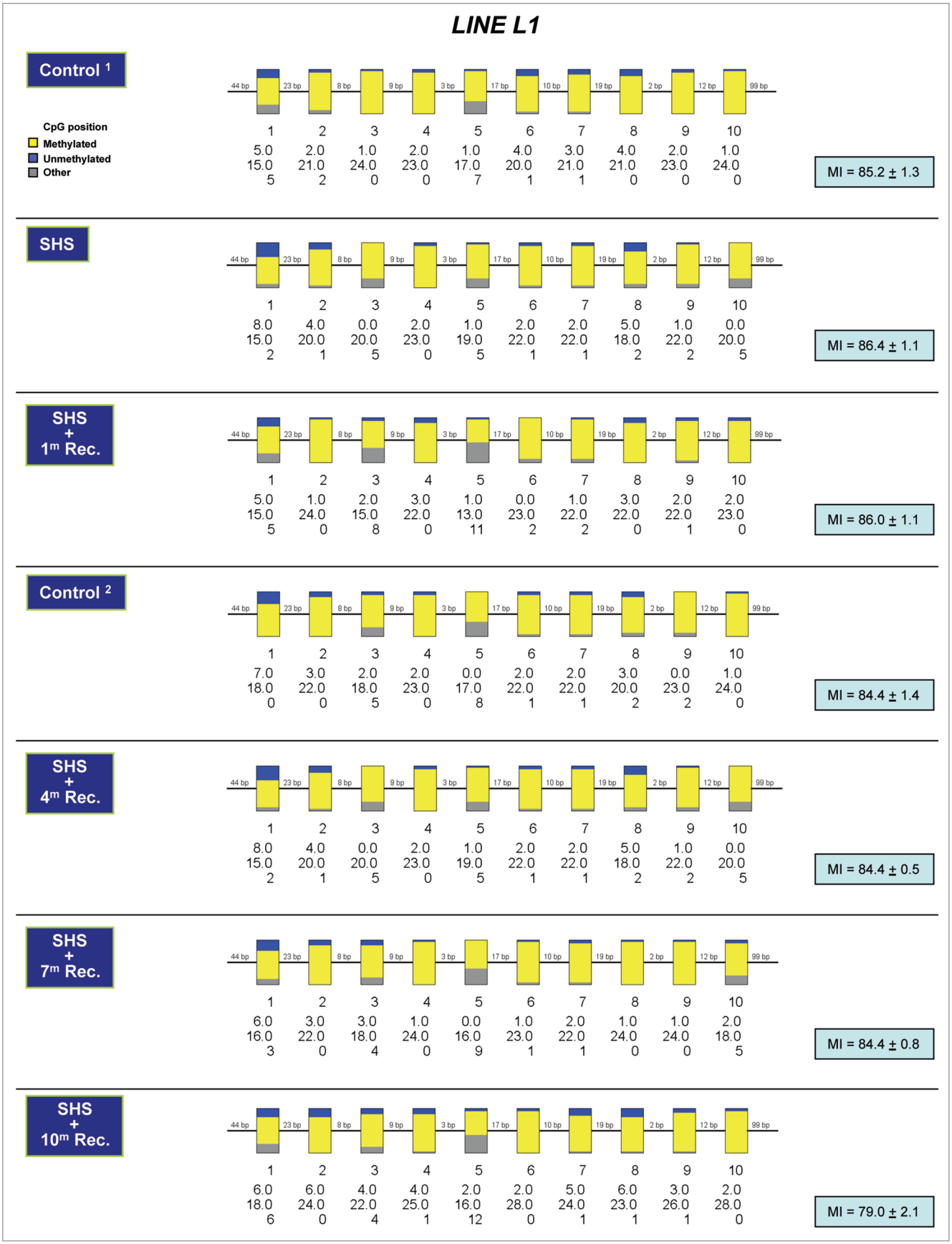

Figure 3. For figure legend, see page 4.

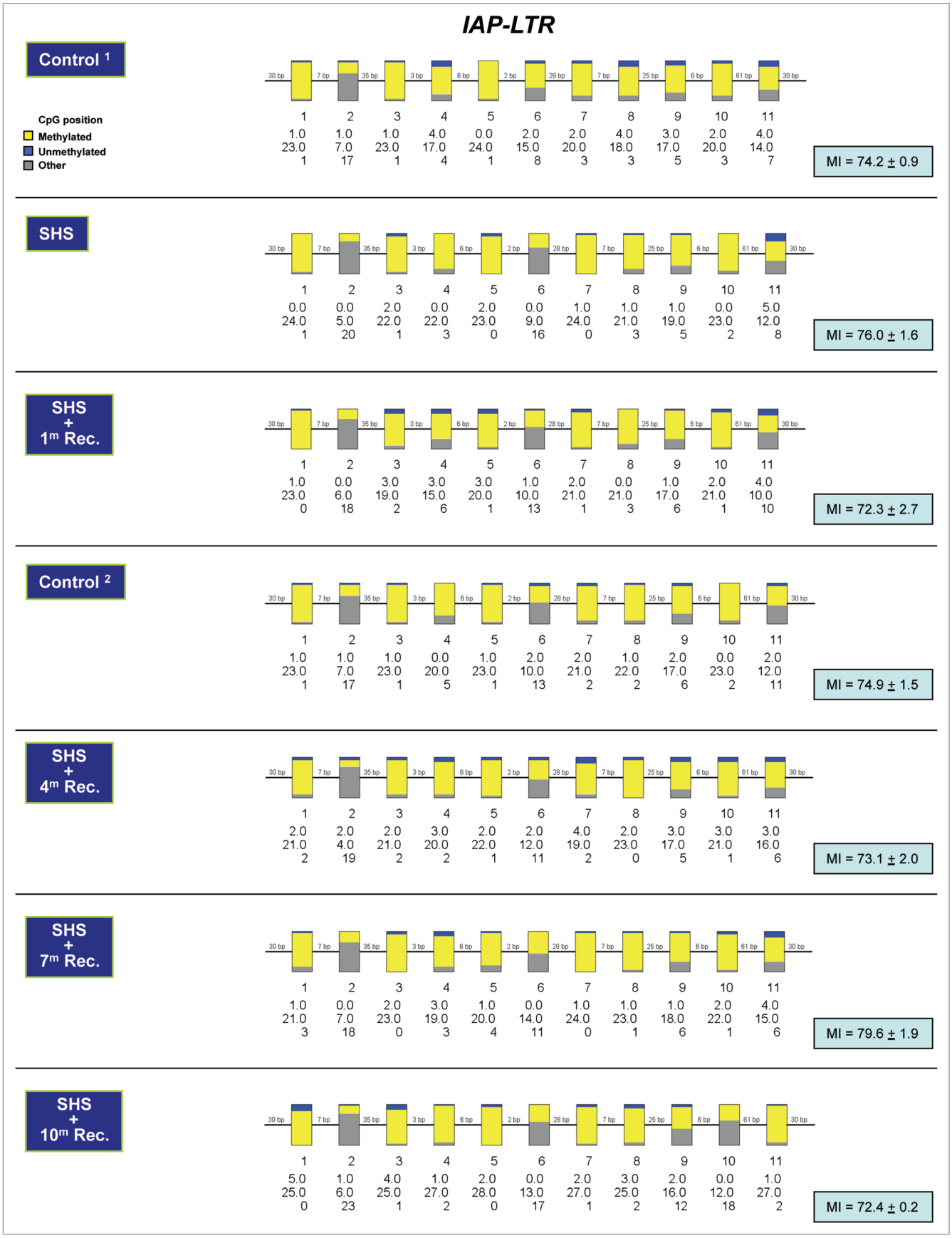

Figure 4. For figure legend, see page 7.

Figure 4 (See opposite page). Methylation profiling of IAP-LTR repetitive DNA elements in SHS-exposed mice vs. control. Bisulfite sequencing of IAP-LTR elements was performed on genomic DNA isolated from the lung of SHS-exposed and control mice using a published protocol.[33] Representative results for samples of SHS-exposed mice (immediately after treatment, and after 1, 4, 7 and 10 mo recovery periods) and control are shown (see legend for **Fig. 3**). Marginal differences in MI between experimental and control mice were not statistically significant (Fisher's exact test).

Lastly, we used a sodium bisulfite-based sequencing analysis[33] to investigate the methylation status of major repetitive DNA elements, including LINE L1, IAP-LTR and SINE B1,[30-32] in the lung of SHS-exposed mice and control. As shown in **Figures 3–5**, the methylation profiles of the LINE L1, IAP-LTR and SINE B1 elements did not change significantly in the lung of any group of mice exposed to SHS relative to control. More specifically, the methylation indices of LINE L1, IAP-LTR and SINE B1 elements in the lung of SHS-exposed mice were not statistically different from those in the lung of control mice (either before or after the recovery periods) (**Figs. 3–5**). Detailed information on the methylation status of each CpG within the LINE L1, IAP-LTR and SINE B1 elements in each mouse in both experimental and control groups are shown in **Figures S3–5**. The overall results indicate that, under the experimental conditions of this study, global DNA hypomethylation does not occur at major repetitive DNA elements in the lung of SHS-exposed mice relative to control.

Discussion

Aberrant DNA methylation is the most established epigenetic mechanism of carcinogenesis.[11-14] Aberration of DNA methylation occurs frequently in lung cancer,[9,10,37-39] with exposure to SHS being a known risk factor.[1-4] The causal relationship between aberrant DNA methylation and lung carcinogenesis in SHS-exposed individuals, however, remains to be determined.[5] In the present study, we have investigated whether SHS can cause changes of DNA methylation in the lung of mice exposed to SHS for a duration of 4 mo, both after the termination of exposure and at ensuing intervals post-exposure (up to 10 mo). Our genome-wide profiling of DNA methylation in the lung of SHS-exposed mice revealed that all groups of SHS-exposed mice and controls shared a similar pattern of DNA methylation (**Fig. 1**). The resemblance of DNA methylomes in SHS-exposed mice and control was confirmed by conventional COBRA and bisulfite sequencing analyses,[28,29] which verified that there were no significant changes in the extent of DNA methylation in any of the analyzed genes between SHS-exposed mice and control (**Fig. 2; Figs. S1 and S2**). Applying a bisulfite-based sequencing approach,[33] we have also demonstrated that the methylation status of major repetitive DNA elements, including LINE L1, IAP-LTR and SINE B1,[30-32] in the lung of all groups of SHS-exposed mice and controls remained comparable (**Figs. 3–5**; **Figs. S3–5**). Thus, the characteristics of aberrant DNA methylation in cancer, which are locus-specific hypermethylation and global hypomethylation of DNA repeats,[11,13,15] were absent in the lung of SHS-exposed mice, both before and after various recovery periods.

Using the same experimental model system and SHS-treatment protocol used in the present study, we have recently demonstrated that SHS can cause persistent genotoxic effects, including DNA damage and mutation, in the lung of SHS-exposed mice.[24,25] The pattern of mutations in the *cII* transgene in the lung of SHS-exposed mice was remarkably similar to that found in the *TP53* gene in lung tumors of nonsmokers.[25] These mechanistic data verify a genotoxic mode of action for SHS of relevance for lung carcinogenesis, and provide proof of evidence on the link between SHS exposure and lung cancer development in nonsmokers. In addition, these experimental findings validate the relevance of our mouse model system and the applied SHS-treatment protocol for studying lung carcinogenesis in vivo. We have further confirmed the validity of this model system and the robustness of the SHS-treatment protocol for investigating lung carcinogenesis by cataloguing gene expression profile (genome-wide) in the lung of SHS-exposed mice (Tommasi et al., ongoing project). Using the Affymetrix gene expression microarray analysis, we have detected a large number of differentially expressed genes in the lung of SHS-exposed mice relative to control (**Fig. 6**). Gene ontology analysis of the differentially expressed transcripts revealed that gene families involved in respiratory disease, genetic disorder and inflammatory disease were highly enriched. Top bio-functional network included gene families that are often affected in cancer. Because DNA methylation is a key regulator of gene expression,[19,20] these transcriptome profiling data further substantiate the usefulness of this model system and the relevance of the applied SHS-treatment protocol for studying DNA methylation, gene regulation, and lung cancer. As mentioned above, however, we were unable to detect any significant changes in the profile of DNA methylation in the lung of SHS-exposed mice, which might have explained the alterations of gene expression found in these animals.

The absence of a prime epigenetic effect, such as aberrant DNA methylation, which could potentially regulate gene expression,[18] in the lung of SHS-exposed mice in this study might be ascribed to various reasons. First, SHS exposure may induce other epigenetic effects, such as histone modifications, chromatin remodeling and microRNA-derived modulation of gene expression,[19,20,40,41] which may, secondarily and upon engagement of a parallel transforming event, result in aberrant DNA methylation. Considering the observed mutagenic effects of SHS,[5,24,25] aberrant DNA methylation may as well be a consequence of mutagenic events that can secondarily influence key pathways involved in establishment and/or maintenance of CpG methylation. A scenario can be envisioned in which SHS-induced genetic and/or epigenetic effects that directly or indirectly modulate DNA methylation, e.g., by up- or down-regulating the expression or activities of DNA methyltransferases or potential demethylase(s), may initiate region-specific DNA hypermethylation and/or global DNA hypomethylation consequent to SHS exposure. One cannot, however, rule out the possibility that longer SHS exposure time or higher concentrations of SHS than those used in the present study might directly induce aberrant DNA methylation.

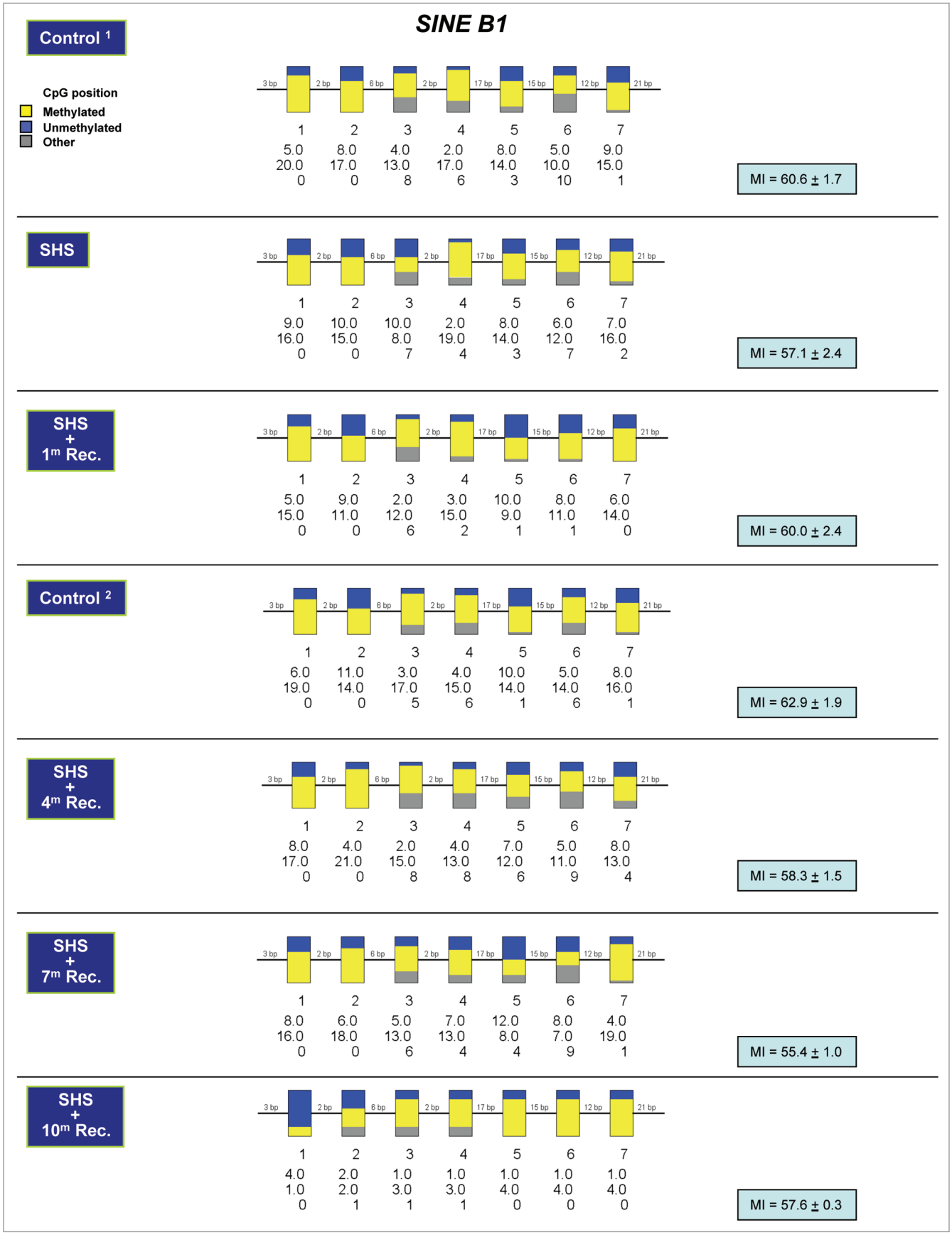

Figure 5. For figure legend, see page 9.

Figure 5 (See opposite page). Methylation profiling of SINE B1 repetitive DNA elements in SHS-exposed mice vs. control. Bisulfite sequencing of SINE B1 elements was performed on genomic DNA isolated from the lung of SHS-exposed and control mice using a published protocol.[33] Representative results for samples of SHS-exposed mice (immediately after treatment, and after 1, 4, 7 and 10 mo recovery periods) and control are shown (see legend for Fig. 3). Marginal differences in MI between experimental and control mice were not statistically significant (Fisher's exact test).

Nevertheless, the possibility that SHS exposure per se does not cause aberrant DNA methylation, at least under the experimental conditions of this study, cannot be excluded.

The duration of SHS exposure in our study, i.e., 4 mo, corresponds to ~11% of the average lifespan of our experimental mice. This, together with the longest latency period, i.e., 10 mo post-SHS exposure, comprises nearly one-third of the entire lifespan of our SHS-exposed mice. Of note, no neoplastic lesions were observed in the lung of any group of SHS-exposed mice by gross examination upon necropsy. Hutt et al.[42] have demonstrated that lifespan whole body exposure of mice to cigarette smoke at a concentration comparable to that used in the present study is required to induce focal alveolar hyperplasias, pulmonary adenomas, papillomas and adenocarcinomas. Our study design, however, partly covered the entire life spectrum of SHS-exposed mice, as our goal was to identify "early" biomarkers of SHS-induced lung carcinogenesis. Logistically, life-long exposure of mice to SHS is extremely demanding and beyond the scope of the present study or our available resources. Nonetheless, the results of our gene expression profiling (**Fig. 6**), together with those of our genotoxicity experiments in this model system,[24,25] confirm that "early" biological effects of SHS exposure of relevance for lung carcinogenesis can be investigated in this mouse model and within the timeframe used here. Although lifespan SHS-exposure of mice is out of the scope of the present study, it can serve other purposes, such as elucidating the "late" biological events that occur during lung tumorigenesis. Our study is, however, informative in as much as it provides a tentative timeframe (i.e., > 4 mo SHS exposure) within which future studies of SHS-induced lung carcinogenesis should investigate "early" biological consequences of exposure to SHS in this or alternative mouse model systems. Lastly, since SHS is a comparatively weak carcinogen,[5,34,43] and lung tumorigenesis requires prolonged periods of SHS exposure and latency,[5] it is likely that longer-term studies than the present one will find the role played by aberrant DNA methylation in the genesis of lung cancer. Of relevance, we found that B(*a*)P, which is a major component of SHS[5,34] and a potent multi-organ carcinogen,[35,36] produces tumors in mice, which show significantly altered DNA methylome, after six weekly treatments followed by ~10 weeks latency period.

In summary, we have demonstrated that in vivo exposure of mice to SHS does not result in aberrant DNA methylation in the lung of SHS-exposed mice within a timeframe that precedes neoplastic-lesion formation. Our findings warrant further research into the underlying mechanism(s) of global loss of DNA methylation and/or locus-specific gain of DNA methylation that may, in turn, contribute to lung carcinogenesis in SHS-exposed nonsmokers. Elucidating the initiating events that cause aberrant DNA methylation in lung cancer may help improve future strategies for prevention, early detection, and treatment of this highly lethal malignancy.

Materials and Methods

Animals. All experiments were conducted in the City of Hope Animal Resources Center, and approved by the Institutional Animal Care and Use Committee in accordance with the recommendations of the National Institutes of Health provided in the Guide for the Care and Use of Laboratory Animals. Detailed information on the Big Blue® mice used in the present study is available in Ref.[24] Briefly, 50 male adult mice were randomly divided into two groups: (1) experimental (SHS exposure; n = 25) and (2) control (clean air mock-exposure; n = 25), each subdivided into five categories (5 mice, each), including (1) four months exposure, (2) four months exposure plus one month recovery, (3) four months exposure plus four months recovery, (4) four months exposure plus seven months recovery, and (5) four months exposure plus ten months recovery. The mice assigned to each experimental or control group were kept in polypropylene cages in groups of 2–3 animals per cage, and housed in an air-conditioned animal room with ambient temperature of 21 ± 1°C and relative humidity of 55% with 12 h light/dark cycle. Throughout all experiments, including the exposure phase and recovery periods, the mice had access to food (PicoLab Rodent Diet 20, PMI Nutrition International, LLC.) and water ad libitum.

Smoking machine and SHS exposure. Detailed information on smoking machine and the protocol for SHS exposure of mice are available in reference 24. Briefly, a custom-made smoking machine (model TE-10, Teague Enterprises) was used to generate SHS for experimental exposure of mice to SHS. All mice assigned to various experimental groups underwent an acclimatization period during which, they were gradually exposed to incremental doses of SHS (see Fig. 1 in ref. 24). Following the acclimatization period, the mice were maintained on a SHS exposure regimen, which consisted of whole body exposure to SHS for 5 h per day, 5 d per week, for a duration of 4 mo. Control mice were handled similarly to SHS-exposed animals, and underwent mock-exposure to filtered high-efficiency particulate-air (HEPA). At the end of all experiments, including the SHS/mock-exposure and various recovery periods, the mice were euthanized by CO_2 asphyxiation, and the lungs were harvested, and genomic DNA was isolated[25] and preserved at -80°C until further analysis.

Genome-wide DNA methylation profiling by MIRA-microarray analysis. We used the MIRA in combination with microarray analysis[26,27] to catalog the DNA methylation profile, on a genome-wide scale, in the lung of SHS-exposed mice. As a pull-down assay for enrichment of the methylated CpG content of DNA, the MIRA is based on the ability of the methyl-CpG binding 2b (MBD2b) protein to bind methylated-CpG dinucleotides, while this reaction is enhanced in the presence of MBD3L1 protein.[44] The MIRA-enriched- and input (non-enriched) DNA

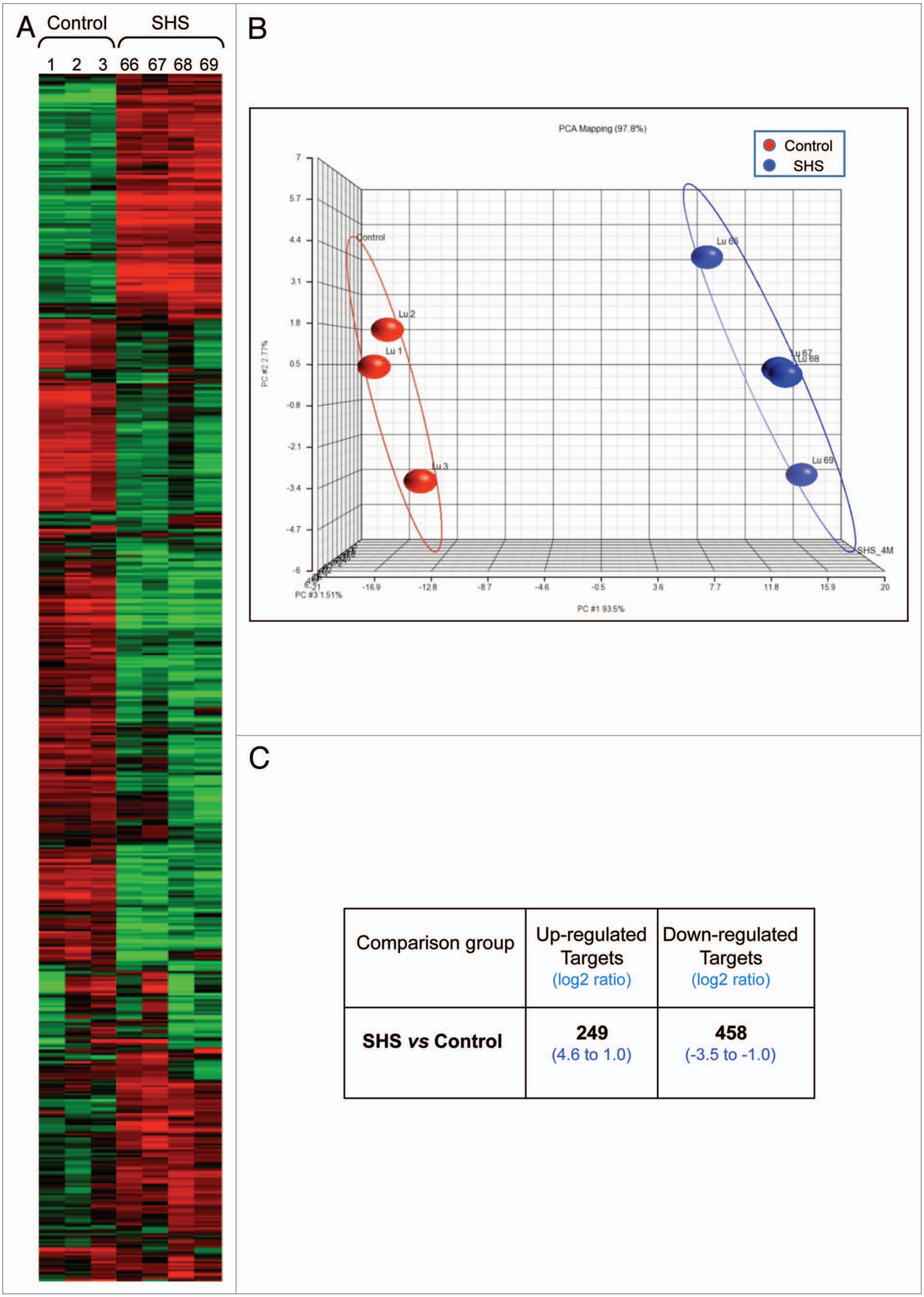

Comparison group	Up-regulated Targets (log2 ratio)	Down-regulated Targets (log2 ratio)
SHS *vs* Control	**249** (4.6 to 1.0)	**458** (-3.5 to -1.0)

Figure 6. For figure legend, see page 11.

Figure 6 (See opposite page). Global gene expression profiling in SHS-exposed mice vs. control. Genome-wide gene expression profiling was performed on RNA samples from SHS-exposed and control mice using the GeneChip® Mouse Genome 430 2.0 Array (Affymetrix Inc.). Representative results from samples of SHS-exposed mice (immediately after 4-mo treatment) and control[1] (6 mo old clean-air mock-treated mice) are shown. (**A**) Heatmap of gene expression profiles in the lung of SHS-exposed mice and control by the Hierarchical Clustering Analysis. Numbers indicate mouse IDs. (**B**) Principal Component Analysis of gene expression profiles in the lung of SHS-exposed mice and control by the Partek Genomics Suite v6.11.1116 (www.partek.com). (**C**) Summary of differentially expressed genes identified in the lung of SHS-exposed mice relative to control. The Bioconductor package "ArrayTool" was used to identify differentially expressed genes in experimental mice vs. control. Genes with significantly different expression levels were selected by using a cutoff p value of < 0.05, and 2-fold change (log2 = 1) in expression level. The number of upregulated- and downregulated genes together with fold-change in expression level (range) in experimental mice vs. control is shown.

fractions can be amplified by polymerase chain reaction (PCR), and subsequently labeled and hybridized to commercially available microarrays to interrogate chromosomal regions of interest or the entire CpG island battery of a genome.[27] Briefly, one microgram of lung genomic DNA from each of the SHS-exposed- and control mice was fragmented by a UCD-200 Bioruptor sonicator (Diagenode Inc.). The sonication set up was 30 sec on/off cycles at medium intensity for a duration of 15 min. The average size of the sonicated DNA fragments, determined by electrophoresis on 1.5% agarose gel, was 300–700 basepairs (bp). Purified GST-tagged MBD2b and His-tagged MBD3L1 proteins (2.5 μg each) were pre-incubated with a solution containing 10 mM TRIS-HCl, pH 7.5, 50 mM NaCl, 1 mM EDTA, 1 mM DTT, 3 mM $MgCl_2$, 0.1% Triton-X100, 5% glycerol, 25 mg/ml BSA and sonicated JM110$^{(dcm-)}$ bacterial DNA (500 ng) for 20 min at 4°C on a rocking platform. The fragmented DNA was then added to the pre-incubated mix, and binding of the MBD2b/MBD3L1 complex to methylated CpGs was achieved after an overnight incubation, as described above. The resultant was mixed with pre-washed MagneGST glutathione particles (Promega), and purified by magnetic capturing according to the manufacturer's instructions. The enriched fraction containing MBD2b/MBD3L-bound methylated CpGs was further processed using the QIAquick PCR purification kit (Qiagen) to elute the methylated CpG content.

Following the enrichment procedure, the CpG-enriched DNA fragments and correspondent non-enriched input DNA (sonicated only) underwent blunt-ending in a reaction mixture of T4 DNA polymerase (New England Biolabs), and subsequently subjected to linker ligation overnight.[27] The ligation products were amplified in a real-time PCR for 16–19 cycles (within the linear range). After purification, the amplicons (1 μg) of the enriched- and input DNA fractions from each sample were labeled with Cy5-dCTP and Cy3-dCTP (Amersham Biosciences, GE Healthcare UK limited), respectively, using a BioPrime Array CGH Genomic Labeling kit (Invitrogen Corp.), and subsequently mixed and hybridized to the Roche NimbleGen Mouse DNA Methylation 3× 720K CpG Island Plus RefSeq Promoter Arrays (Roche NimbleGen Inc.). This microarray platform covers important regulatory elements, including 20,404 RefSeq gene promoters, and 15,988 annotated CpG islands. The microarray slides were scanned using an Agilent Scanner (Agilent Technologies Inc.), and images were quantified by NimbleScan v2.5 (Roche NimbleGen, Inc.). The raw microarray data have been deposited in the National Center for Biotechnology Information Gene Expression Omnibus database, and the accession number is GSE41421.

Processing and analysis of the MIRA-microarray data. The raw intensity of probes was normalized by Loess normalization within each array and the resulting log2 ratio data were further quantile normalized across all the arrays. Probes were selected as positive if their normalized log2 ratio was above 1 (2-fold). For our analysis, we defined a methylated region of interest (methylation peak) as a region with at least four consecutive positive probes, allowing one probe gap, covering a minimum length of 350 bp. This stringent definition will help preclude false-positive results. Identified methylation peaks were mapped to known transcripts defined in the UCSC Genome Browser MM9 RefSeq database (http://hgdownload.cse.ucsc.edu/goldenPath/mm9/database/). Methylation peaks falling into 1,000 bp relative to transcription start sites were defined as upstream peaks; methylation peaks falling within 1,000 bp of RefSeq transcript end sites were defined as downstream peaks, and those falling within gene bodies (from 1,000 bp downstream of transcription start to 1,000 bp upstream of transcript end) were defined as "intragenic" peaks. Methylation peaks that were not close to any known transcripts were defined as "intergenic."

Methylation peaks in samples from SHS-treated mice and control were identified as above. The methylated regions in samples from SHS-treated mice were matched by outer join, and their methylation status was determined by the presence of methylation peaks in each sample in these matched regions. Only the regions methylated in all samples from each group of SHS-treated mice and unmethylated in samples from correspondent control mice were considered as hypermethylated candidates. The average log2 ratios of probes within these candidates in samples from SHS-treated mice were compared with the average log2 ratios of probes in samples from control mice, and the final SHS-specific hypermethylation peaks were selected if the difference was more than 1 (over 2-fold). Conversely, hypomethylated candidates in samples from SHS-treated mice were selected as those in which methylation peaks were present in all samples from control mice but absent in samples from correspondent SHS-treated mice, and the average probe log2 ratio was > 1 (> 2-fold).

Single gene DNA methylation analysis by COBRA and bisulfite genomic sequencing. We verified the methylation status of individual target genes identified by MIRA-microarray analysis in samples from SHS-exposed mice as compared with control using conventional COBRA,[28] and sodium bisulfite genomic sequencing.[29] Briefly, one microgram of genomic DNA was subjected to sodium bisulfite treatment using the Qiagen EpiTect kit according to the manufacturer's instructions (Qiagen). The purified bisulfite-treated DNA was analyzed by standard COBRA using specific sets of primers designed for each target gene.[28] The

primer sequences used for PCR amplification of all the analyzed targets are available upon request. Mouse genomic DNA, isolated from the lung, was methylated in vitro with M. SssI CpG methyltransferase (New England Biolabs), and served as control. For genomic sequencing, the PCR products obtained after bisulfite conversion of genomic DNA were cloned into the TOPO-TA cloning vector according to the manufacturer's instructions (Invitrogen Inc.). Randomly selected clones from each SHS-treated mouse and control were then sequenced using an ABI-3730 DNA Sequencer (ABI Prism, PE Applied BioSystems).

DNA methylation analysis of repetitive DNA elements. To determine whether global loss of DNA methylation occurs consequent to SHS exposure, we have also investigated the methylation status of major repetitive DNA elements, including LINE L1, IAP-LTR, SINE B1,[30-32] in the lung of SHS-exposed mice using a bisulfite-based genomic sequencing analysis.[33] We adapted a published procedure,[33] which involves sodium-bisulfite treatment of the genomic DNA, followed by primer amplification of the consensus sequences from the respective elements, and direct DNA sequencing of PCR products. Evolutionarily, methylated CpGs on the forward- or reverse strands of these elements can undergo spontaneous deamination of 5-methylcytosine to thymine, thereby mutating to 5'-TpG-3' or 5'-CpA-3', respectively. Dependent on the status of cytosine methylation, non-mutated CpGs can be converted to 5'-TpG-3' (if unmethylated) or remain unchanged (if methylated) after bisulfite treatment of DNA in vitro.[33] Thus, direct DNA sequencing of the bisulfite-treated and PCR-amplified fragments derived from these elements can provide detailed information on the status of CpG methylation and mutation in these elements.[27,33] **Table S1** provides information on the genomic sequence and primer design of the repetitive DNA elements analyzed in the present study. Sodium bisulfite genomic sequencing was performed as described above, with randomly selected clones from all the SHS-treated mice and control.

Disclosure of Potential Conflicts of Interest

No potential conflicts of interest were disclosed.

Acknowledgments

We would like to thank Dr Yong Jiang for technical assistance in the conduct of SHS-exposure experiments, Dr Fong-Fong Chu for help with mouse breeding and colony expansion, and Dr Walter Tsark for helpful discussion on IACUC protocol preparation. Special thanks to the dedicated staff and management of the City of Hope Animal Resources Center, in particular, Armando Amaya, Marie Prez, Lauren Ratcliffe, Yvonne Harper, Donna Isbell, Kenneth Golding, and Dr Richard Ermel. Work of the authors is supported by grants from the American Cancer Society (RSG-11-083-01-CNE) and the University of California Tobacco Related Disease Research Program (18KT-0040 and 20XT-0116) to A.B. None of the authors have conflicts of interest that might be construed to influence the results or interpretation of the data presented in this manuscript. The sponsors of the study had no role in study design, data collection, data analysis, data interpretation, writing of the report, or in the decision to submit for publication. The corresponding author had full access to all the data in the study and had final responsibility for the decision to submit for publication.

Supplemental Materials

Supplemental materials may be found here:
www.landesbioscience.com/journals/epigenetics/article/22453

References

1. International Agency for Research on Cancer (IARC). Tobacco smoke and involuntary smoking. Lyon: World Health Organization (WHO), International Agency for Research on Cancer, 2004: 1191-413.
2. The US Surgeon General. The health consequences of involuntary exposure to tobacco smoke: A report of the Surgeon General. US Department of Health and Human Services, Centers for Disease Control and Prevention, Coordinating Center for Health Promotion, National Center for Chronic Disease Prevention and Health Promotion, Office on Smoking and Health, 2006.
3. World Health Organization (WHO). WHO report on the global tobacco epidemic: the MPOWER package, 2008.
4. Oberg M, Jaakkola MS, Woodward A, Peruga A, Prüss-Ustün A. Worldwide burden of disease from exposure to second-hand smoke: a retrospective analysis of data from 192 countries. Lancet 2011; 377:139-46; PMID:21112082; http://dx.doi.org/10.1016/S0140-6736(10)61388-8.
5. Besaratinia A, Pfeifer GP. Second-hand smoke and human lung cancer. Lancet Oncol 2008; 9:657-66; PMID:18598930; http://dx.doi.org/10.1016/S1470-2045(08)70172-4.
6. Wipfli HL, Samet JM. Second-hand smoke's worldwide disease toll. Lancet 2011; 377:101-2; PMID:21112081; http://dx.doi.org/10.1016/S0140-6736(10)61922-8.
7. Jemal A, Bray F, Center MM, Ferlay J, Ward E, Forman D. Global cancer statistics. CA Cancer J Clin 2011; 61:69-90; PMID:21296855; http://dx.doi.org/10.3322/caac.20107.
8. American Cancer Society (ACS). Cancer facts & figures 2012. American Cancer Society Inc.: National Home Office. Atlanta: American Cancer Society, 2012.
9. Sato M, Shames DS, Gazdar AF, Minna JD. A translational view of the molecular pathogenesis of lung cancer. J Thorac Oncol 2007; 2:327-43; PMID:17409807; http://dx.doi.org/10.1097/01.JTO.0000263718.69320.4c.
10. Sun S, Schiller JH, Gazdar AF. Lung cancer in never smokers--a different disease. Nat Rev Cancer 2007; 7:778-90; PMID:17882278; http://dx.doi.org/10.1038/nrc2190.
11. Kulis M, Esteller M. DNA methylation and cancer. Adv Genet 2010; 70:27-56; PMID:20920744; http://dx.doi.org/10.1016/B978-0-12-380866-0.60002-2.
12. Laird PW. Principles and challenges of genome-wide DNA methylation analysis. Nat Rev Genet 2010; 11:191-203; PMID:20125086; http://dx.doi.org/10.1038/nrg2732.
13. Baylin SB, Jones PA. A decade of exploring the cancer epigenome - biological and translational implications. Nat Rev Cancer 2011; 11:726-34; PMID:21941284; http://dx.doi.org/10.1038/nrc3130.
14. Rodríguez-Paredes M, Esteller M. Cancer epigenetics reaches mainstream oncology. Nat Med 2011; 17:330-9; PMID:21386836; http://dx.doi.org/10.1038/nm.2305.
15. Laird PW. The power and the promise of DNA methylation markers. Nat Rev Cancer 2003; 3:253-66; PMID:12671664; http://dx.doi.org/10.1038/nrc1045.
16. Feinberg AP, Vogelstein B. Hypomethylation distinguishes genes of some human cancers from their normal counterparts. Nature 1983; 301:89-92; PMID:6185846; http://dx.doi.org/10.1038/301089a0.
17. Wilson AS, Power BE, Molloy PL. DNA hypomethylation and human diseases. Biochim Biophys Acta 2007; 1775:138-62; PMID:17045745.
18. Esteller M. Epigenetics in cancer. N Engl J Med 2008; 358:1148-59; PMID:18337604; http://dx.doi.org/10.1056/NEJMra072067.
19. Suzuki MM, Bird A. DNA methylation landscapes: provocative insights from epigenomics. Nat Rev Genet 2008; 9:465-76; PMID:18463664; http://dx.doi.org/10.1038/nrg2341.
20. Jones PA, Baylin SB. The epigenomics of cancer. Cell 2007; 128:683-92; PMID:17320506; http://dx.doi.org/10.1016/j.cell.2007.01.029.
21. Takai D, Jones PA. Comprehensive analysis of CpG islands in human chromosomes 21 and 22. Proc Natl Acad Sci U S A 2002; 99:3740-5; PMID:11891299; http://dx.doi.org/10.1073/pnas.052410099.
22. Ehrlich M. DNA hypomethylation in cancer cells. Epigenomics 2009; 1:239-59; PMID:20495664; http://dx.doi.org/10.2217/epi.09.33.
23. Nagarajan RP, Costello JF. Epigenetic mechanisms in glioblastoma multiforme. Semin Cancer Biol 2009; 19:188-97; PMID:19429483; http://dx.doi.org/10.1016/j.semcancer.2009.02.005.
24. Kim SI, Arlt VM, Yoon JI, Cole KJ, Pfeifer GP, Phillips DH, et al. Whole body exposure of mice to secondhand smoke induces dose-dependent and persistent promutagenic DNA adducts in the lung. Mutat Res 2011; 716:92-8; PMID:21925188; http://dx.doi.org/10.1016/j.mrfmmm.2011.08.008.

25. Kim SI, Yoon JI, Tommasi S, Besaratinia A. New experimental data linking secondhand smoke exposure to lung cancer in nonsmokers. FASEB J 2012; 26:1845-54; PMID:22318968; http://dx.doi.org/10.1096/fj.11-199984.
26. Tommasi S, Karm DL, Wu X, Yen Y, Pfeifer GP. Methylation of homeobox genes is a frequent and early epigenetic event in breast cancer. Breast Cancer Res 2009; 11:R14; PMID:19250546; http://dx.doi.org/10.1186/bcr2233.
27. Tommasi S, Kim SI, Zhong X, Wu X, Pfeifer GP, Besaratinia A. Investigating the epigenetic effects of a prototype smoke-derived carcinogen in human cells. PLoS One 2010; 5:e10594; PMID:20485678; http://dx.doi.org/10.1371/journal.pone.0010594.
28. Xiong Z, Laird PW. COBRA: a sensitive and quantitative DNA methylation assay. Nucleic Acids Res 1997; 25:2532-4; PMID:9171110; http://dx.doi.org/10.1093/nar/25.12.2532.
29. Frommer M, McDonald LE, Millar DS, Collis CM, Watt F, Grigg GW, et al. A genomic sequencing protocol that yields a positive display of 5-methylcytosine residues in individual DNA strands. Proc Natl Acad Sci U S A 1992; 89:1827-31; PMID:1542678; http://dx.doi.org/10.1073/pnas.89.5.1827.
30. Waterston RH, Lindblad-Toh K, Birney E, Rogers J, Abril JF, Agarwal P, et al.; Mouse Genome Sequencing Consortium. Initial sequencing and comparative analysis of the mouse genome. Nature 2002; 420:520-62; PMID:12466850; http://dx.doi.org/10.1038/nature01262.
31. Goodier JL, Ostertag EM, Du K, Kazazian HH Jr. A novel active L1 retrotransposon subfamily in the mouse. Genome Res 2001; 11:1677-85; PMID:11591644; http://dx.doi.org/10.1101/gr.198301.
32. Martens JH, O'Sullivan RJ, Braunschweig U, Opravil S, Radolf M, Steinlein P, et al. The profile of repeat-associated histone lysine methylation states in the mouse epigenome. EMBO J 2005; 24:800-12; PMID:15678104; http://dx.doi.org/10.1038/sj.emboj.7600545.
33. Yang AS, Estécio MR, Doshi K, Kondo Y, Tajara EH, Issa JP. A simple method for estimating global DNA methylation using bisulfite PCR of repetitive DNA elements. Nucleic Acids Res 2004; 32:e38; PMID:14973332; http://dx.doi.org/10.1093/nar/gnh032.
34. Hecht SS. Tobacco carcinogens, their biomarkers and tobacco-induced cancer. Nat Rev Cancer 2003; 3:733-44; PMID:14570033; http://dx.doi.org/10.1038/nrc1190.
35. Martin KR, Jokinen MP, Honeycutt HP, Quinn A, Kari FW, Barrett JC, et al. Tumor profile of novel p53 heterozygous Tg.AC (v-Ha-ras) bitransgenic mice treated with benzo(a)pyrene and fed dietary N-acetyl-L-cysteine (NAC). Toxicological sciences: an official journal of the Society of Toxicology 2004; 81:293-301.
36. Talaska G, Jaeger M, Reilman R, Collins T, Warshawsky D. Chronic, topical exposure to benzo[a]pyrene induces relatively high steady-state levels of DNA adducts in target tissues and alters kinetics of adduct loss. Proc Natl Acad Sci U S A 1996; 93:7789-93; PMID:8755554; http://dx.doi.org/10.1073/pnas.93.15.7789.
37. Belinsky SA. Gene-promoter hypermethylation as a biomarker in lung cancer. Nat Rev Cancer 2004; 4:707-17; PMID:15343277; http://dx.doi.org/10.1038/nrc1432.
38. Heller G, Zielinski CC, Zöchbauer-Müller S. Lung cancer: from single-gene methylation to methylome profiling. Cancer Metastasis Rev 2010; 29:95-107; PMID:20099008; http://dx.doi.org/10.1007/s10555-010-9203-x.
39. Scesnaite A, Jarmalaite S, Mutanen P, Anttila S, Nyberg F, Benhamou S, et al. Similar DNA methylation pattern in lung tumours from smokers and never-smokers with second-hand tobacco smoke exposure. Mutagenesis 2012; 27:423-9; PMID:22217548; http://dx.doi.org/10.1093/mutage/ger092.
40. Esteller M. Cancer epigenomics: DNA methylomes and histone-modification maps. Nat Rev Genet 2007; 8:286-98; PMID:17339880; http://dx.doi.org/10.1038/nrg2005.
41. Schembri F, Sridhar S, Perdomo C, Gustafson AM, Zhang X, Ergun A, et al. MicroRNAs as modulators of smoking-induced gene expression changes in human airway epithelium. Proc Natl Acad Sci U S A 2009; 106:2319-24; PMID:19168627; http://dx.doi.org/10.1073/pnas.0806383106.
42. Hutt JA, Vuillemenot BR, Barr EB, Grimes MJ, Hahn FF, Hobbs CH, et al. Life-span inhalation exposure to mainstream cigarette smoke induces lung cancer in B6C3F1 mice through genetic and epigenetic pathways. Carcinogenesis 2005; 26:1999-2009; PMID:15944214; http://dx.doi.org/10.1093/carcin/bgi150.
43. DeMarini DM. Genotoxicity of tobacco smoke and tobacco smoke condensate: a review. Mutat Res 2004; 567:447-74; PMID:15572290; http://dx.doi.org/10.1016/j.mrrev.2004.02.001.
44. Jiang CL, Jin SG, Pfeifer GP. MBD3L1 is a transcriptional repressor that interacts with methyl-CpG-binding protein 2 (MBD2) and components of the NuRD complex. J Biol Chem 2004; 279:52456-64; PMID:15456747; http://dx.doi.org/10.1074/jbc.M409149200.

Landes Bioscience www.landesbioscience.com

Supplemental Material to:

Stella Tommasi, Albert Zheng, Jae-In Yoon, Arthur Xuejun Li, Xiwei Wu and Ahmad Besaratinia

Whole DNA methylome profiling in mice exposed to secondhand smoke

Epigenetics 2012; 7(11)
http://dx.doi.org/10.4161/epi.22453

http://www.landesbioscience.com/journals/epigenetics/article/22453

TABLE S1: Detailed information on genomic sequences and primer designs for the repetitive DNA elements analyzed by sodium bisulfite DNA sequencing.

Long interspersed nuclear element L1 (LINE L1)				
Original DNA sequence	5'GCCAGAGA*ACCTGACAGCTTCTGGAACAGGCAGAAGCACAGAGGCGCTGAGGCAGCACCCTGTGTG GGCCAGGGACAGCCGGCCACCTTCCGGACCGGAGGACAGGTGCCCACCCGGCTGGGGAGGCGGCCTA AGCCACAGCAGCAGCGGTCGCCATCTTGGTCCCGGGACTCCAAGGAACTTAGGAATTTAGTCTGCTTA GGTGAGAGTCTGTACCACCTGGGAACTGCCAAAGCAACACAGTGTCTGAGAAAGGTCCTGTTTTG3'			
DNA sequence after bisulfite treatment	5'GTTAGAGA*ATTTGATAGTTTTTGGAATAGGTAGAAGTATAGAGGCGTTGAGGTAGTATTTTGTGTGG GTTAGGGATAGTCGGTTATTTTTCGGATCGGAGGATAGGTGTTTATTCGGTTGGGGAGGCGGTTTAAG TTATAGTAGTAGCGGTCGTTATTTTGGTTTCGGGATTTTAAGGAATTTAGGAATTTAGTTTGTTTAGGT GAGAGTTTGTATTATTTGGGAATTGTTAAAGTAATATAGTGTTTGAGAAAGGTTTTGTTTTG3'			
Forward primer	**Designation:** Line1-F	**t_m (°C):** 54.2	**# Bases:** 30	**Sequence:** 5'-GTTAGAGGATTTGATAGTTTTTGGAATAGG-3'
Reverse primer	**Designation:** Line1-R	**t_m (°C):** 54.8	**# Bases:** 30	**Sequence:** 5'-CCAAAACAAAACCTTTCTCAAACACTATAT-3'
PCR product size	266 bp			
# CpGs in PCR product	9			
Interacesternal A particle long terminal repeat retrotransposons (IAP-LTR)				

Original DNA sequence	**5'CTGTGTTCTAAGTGGTAAACAAATAATCTGCGCATATGCCGAGGGTGGTTCTCTACTCCATGTGCTCT GCCTTCCCCGTGACGTCAACTCGGCCGATGGGCTGCAGCCAATCAGGGAGTGACACGTCCTAGGCGAA ATATAACTCTCCTAAAAAAGGGACGGGGTTTCGTTTTCTCTCTCTCTTGCTTCTTACACTCTTGCTCCTG AAGATGTAAGCAATAAAGTTTTGCCGCAGAAGATTCTGGTCTGTGG*TGTTCTTCCT3'**			
DNA sequence after bisulfite treatment	**5'TTGTGTTTTAAGTGGTAAATAAATAATTTGCGTATATGTCGAGGGTGGTTTTTTATTTTATGTGTTTTG TTTTTTTCGTGACGTTAATTCGGTCGATGGGTTGTAGTTAATTAGGGAGTGATACGTTTTAGGCGAAAT ATAATTTTTTTAAAAAAGGGACGGGGTTTCGTTTTTTTTTTTTTTTGTTTTTTATATTTTTGTTTTTGAAG ATGTAAGTAATAAAGTTTTGTCGTAGAAGATTTTGGTTTGTGG*TGTTTTTTTT3'**			
Forward primer	**Designation:** **Iap-F**	**t_m (°C):** **50.6**	**# Bases:** **30**	**Sequence:** **5'-TTGTGTTTTAAGTGGTAAATAAATAATTTG-3'**
Reverse primer	**Designation:** **Iap-R**	**t_m (°C):** **50.3**	**# Bases:** **24**	**Sequence:** **5'-CAAAAAAAACACACAAACCAAAAT-3'**
PCR product size	**263 bp**			
# CpGs in PCR product	**11**			
Short interspersed nuclear element B1 (SINE B1)				
Original DNA sequence	**5'AGCCGGGCGTGGTGGCGCACGCCTTTAATCCCAGCACTCGGGAGGCAGAGGCAGGCGGATTTCTGA GTTCGAGGCCAGCCTGGTCTACAAAG3'**			
DNA sequence after bisulfite treatment	**5'AGTY*GGGY*GTGGTGGCGTACGTTTTTAATTTTAGTATTCGGGAGGTAGAGGTAGGCGGATTTTTGA GTTCGAGGTTAGTTTGGTTTATAAAG3'**			
Forward primer	**Designation:** **SineB1-F**	**t_m (°C):** **55**	**# Bases:** **15**	**Sequence:** **5'-AGTY*GGGY*GTGGTGG-3'**
Reverse primer	**Designation:**	**t_m (°C):**	**# Bases:**	**Sequence:**

	SineB1-R	**46.9**	**22**	**5’-CTTTATAAACCAAACTAACCTC-3’**
PCR product size	**92 bp**			
# CpGs in PCR product	**7**			

- CpG sites are underlined.

- Primer directions are indicated by arrow in the DNA sequence.

-A* = SNP from Guanine to Adenine in LINE L1 where 5’ primer binds

-G* = Insertion of an extra Guanine base in downstream IAP-LTR region flanked by 3’ primer.

-Y* = Base that could be either Thymine or Cytosine for unbiased results in SINE B1_Mm bisulfite sequencing, where two CpG sites were incorporated into 5’ primer.

"SUPPLEMENTARY FIGURE LEGENDS"

Figure S1

Detailed methylation map for each CpG within the *Cacna1s* CpG island in SHS-exposed mice *versus* control.

The extent of CpG methylation within the *Cacna1s* CpG island was determined in the lung genomic DNA from SHS-exposed and control mice using the bisulfite sequencing analysis. Based on microarray data, samples of SHS-exposed mice, which showed the highest hypermethylation in the specified CpG island, were subjected to bisulfite genomic sequencing. The sequencing results of randomly selected independent clones from both the experimental and control mice were analysed using the **QU**antification tool for **M**icroarray **A**nalysis (QUMA) (http://quma.cdb.riken.jp/). Open and closed circles represent unmethylated and methylated CpG dinucleotides, respectively. Percentage of methylation in the *Cacna1s* CpG island for each mouse in both experimental and control groups is shown. Numbers indicate mouse IDs (*e.g.*, # 1, #2, #3, etc). Average results per experimental or control groups are shown as Methylation Index (MI = mean ± SD; calculated by the BIQ Analyzer software (http://biq-analyzer.bioinf.mpi-inf.mpg.de/)). Marginal difference in MI between experimental and control mice was not statistically significant (Fisher's exact test).

Figure S2

Detailed methylation map for each CpG within the *H2-T23* CpG island in SHS-exposed mice *versus* control.

The extent of CpG methylation within the *H2-T23* CpG island was determined in the lung genomic DNA from SHS-exposed and control mice using the bisulfite sequencing analysis. Based on microarray data, samples of SHS-exposed mice, which showed the highest hypomethylation in the specified CpG island, were subjected to bisulfite genomic sequencing (*see*, legend for Fig. S1). Marginal difference in MI between experimental and control mice was not statistically significant (Fisher's exact test).

Figure S3

Detailed methylation map for each CpG within the LINE L1 repetitive DNA elements in SHS-exposed mice *versus* control.

The extent of CpG methylation within the LINE L1 elements was determined in the lung genomic DNA from SHS-exposed and control mice using a bisulfite-based sequencing analysis (*see*, Materials and Methods). The sequencing results of randomly selected independent clones from both experimental and control mice were analysed using the QUMA software (*see*, legend for Fig. S1). Marginal differences in MI between various groups of experimental and control mice were not statistically significant (Fisher's exact test).

Figure S4

Detailed methylation map for each CpG within the IAP-LTR repetitive DNA elements in SHS-exposed mice *versus* control.

The extent of CpG methylation within the IAP-LTR elements was determined in the lung genomic DNA from SHS-exposed and control mice using a bisulfite-based sequencing analysis (*see*, Materials and Methods). The sequencing results of randomly selected independent clones from both experimental and control mice were analysed using the QUMA software (*see*, legend for Fig. S1). Marginal differences in MI between various groups of experimental and control mice were not statistically significant (Fisher's exact test).

Figure S5

Detailed methylation map for each CpG within the SINE B1 repetitive DNA elements in SHS-exposed mice *versus* control.

The extent of CpG methylation within the SINE B1 elements was determined in the lung genomic DNA from SHS-exposed and control mice using a bisulfite-based sequencing analysis (*see*, Materials and Methods). The sequencing results of randomly selected independent clones from both experimental and control mice were analysed using the QUMA software (*see*, legend for Fig. S1). Marginal differences in MI between various groups of experimental and control mice were not statistically significant (Fisher's exact test).

Cacna1s

Control[2]

 # 205

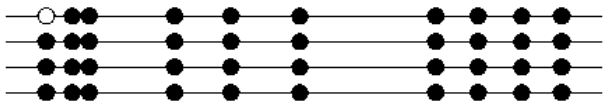

(97.5%)

 # 206

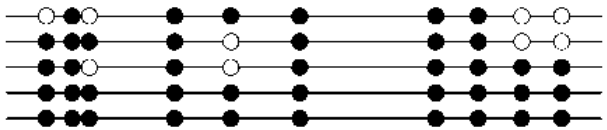

(82.0%)

 # 207

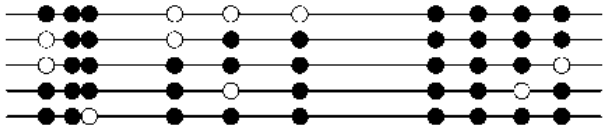

(80.0%)

 # 208

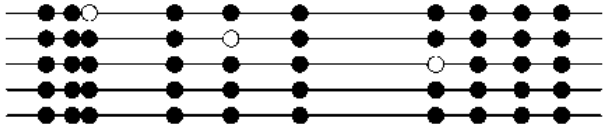

(94.0%)

 # 212

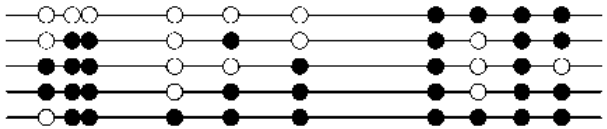

(66.0%)

MI = 83.3 ± 2.1

SHS + 7[m] Rec.

 # 86

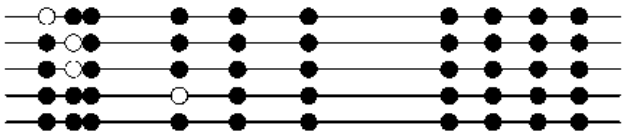

(92.0%)

 # 87

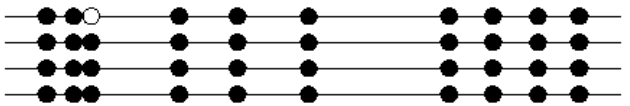

(97.5%)

 # 88

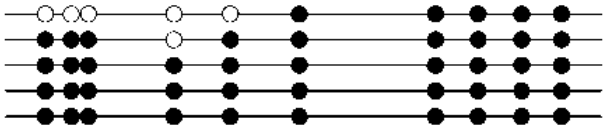

(88.0%)

 # 89

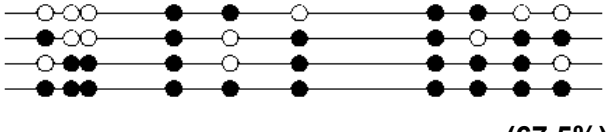

(67.5%)

 # 94

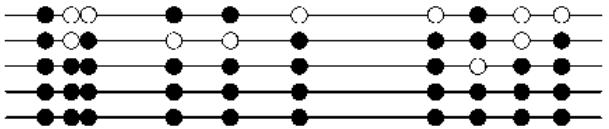

(78.0%)

MI = 84.8 ± 3.2

Fig. S1

H2-T23

Control[1]

 # 1

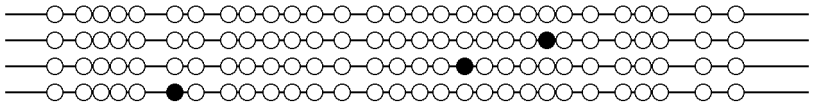

(2.6%)

 # 2

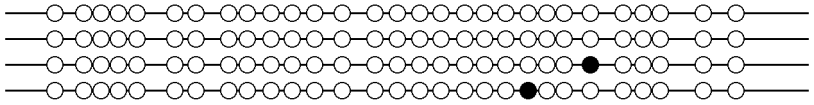

(2.0%)

 # 3

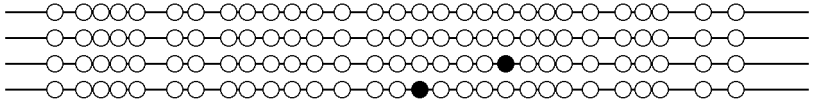

(4.1%)

 # 4

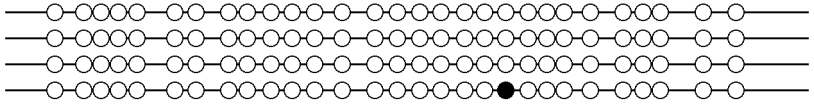

(0.9%)

 # 287

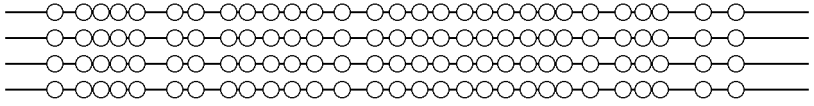

(0.7%)

MI = 2.1 ± 0.3

SHS

 # 66

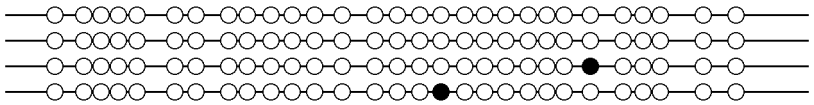

(2.0%)

 # 67

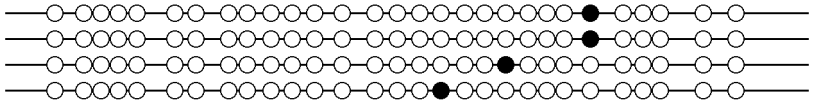

(3.4%)

 # 68

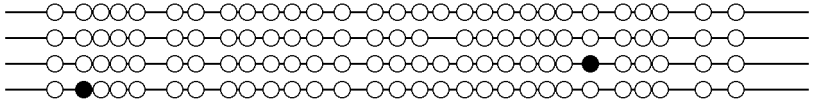

(2.7%)

 # 69

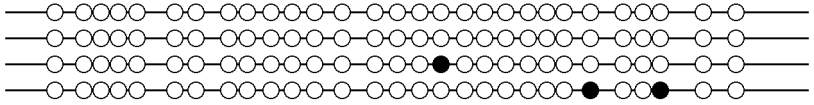

(2.6%)

 # 75

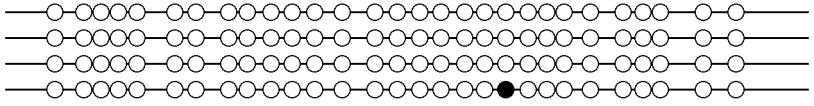

(1.4%)

MI = 2.4 ± 0.2

Fig. S2

LINE L1

Control [1] — MI = 85.2 ± 1.3

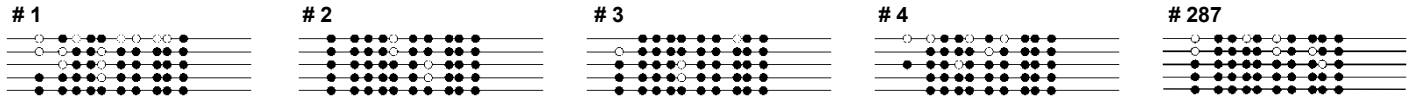

SHS — MI = 86.4 ± 1.1

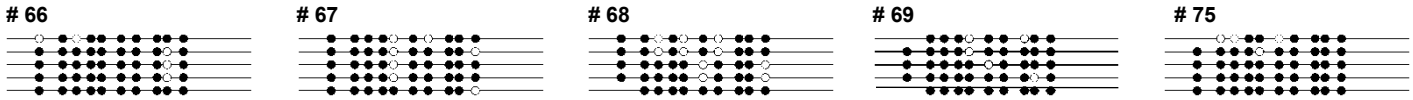

SHS + 1[m] Rec. — MI = 86.0 ± 1.1

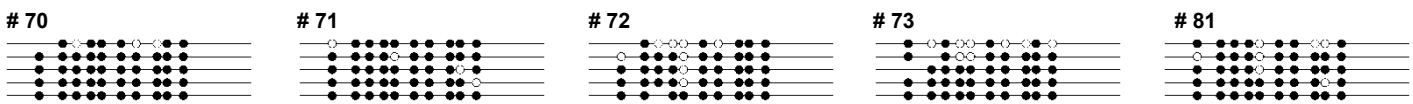

Control [2] — MI = 84.4 ± 1.4

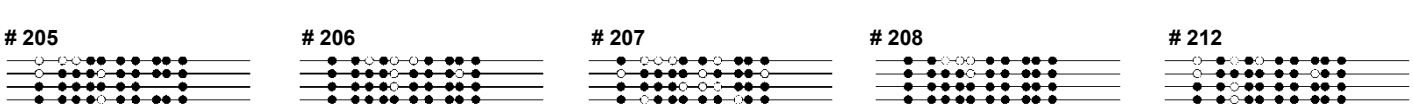

SHS + 4[m] Rec. — MI = 84.4 ± 0.5

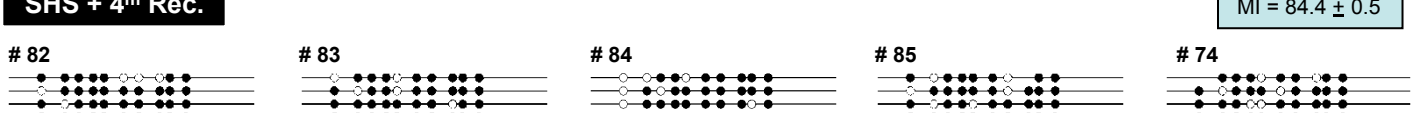

SHS + 7[m] Rec. — MI = 84.4 ± 0.8

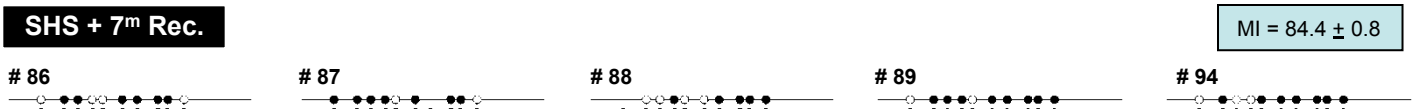

SHS + 10[m] Rec. — MI = 79.0 ± 2.1

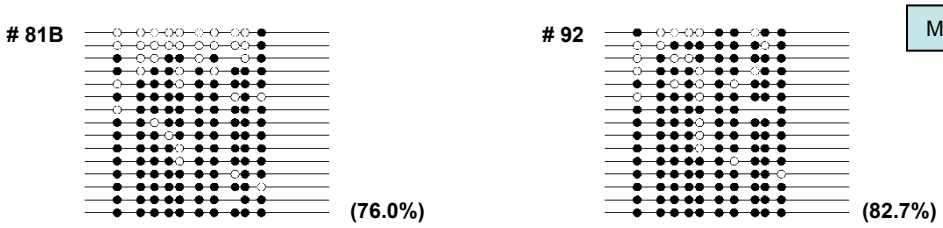

Fig. S3

IAP-LTR

Control [1] — MI = 74.2 ± 0.9

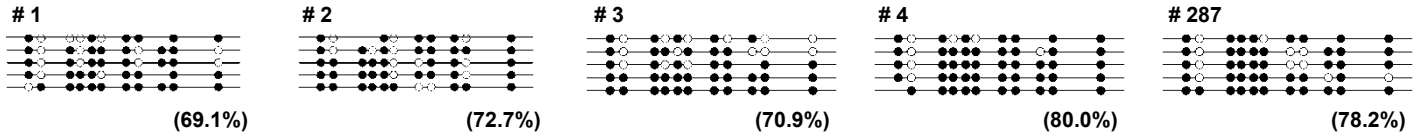

SHS — MI = 76.0 ± 1.6

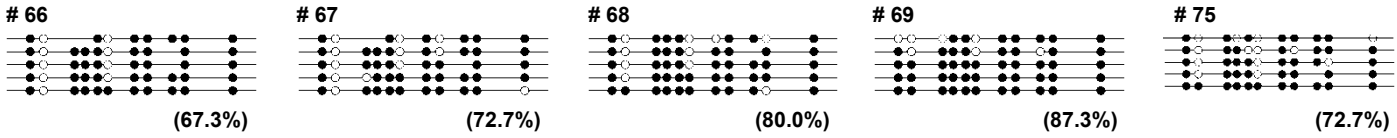

SHS + 1[m] Rec. — MI = 72.3 ± 2.7

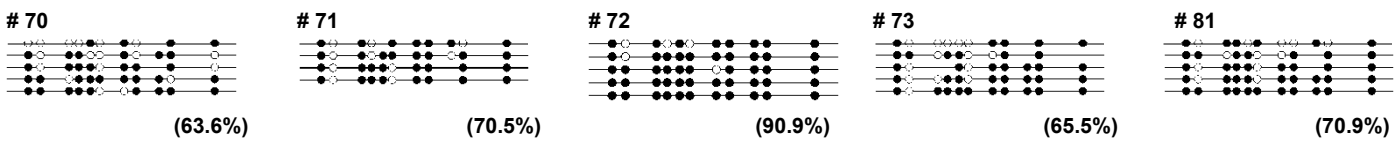

Control [2] — MI = 74.9 ± 1.5

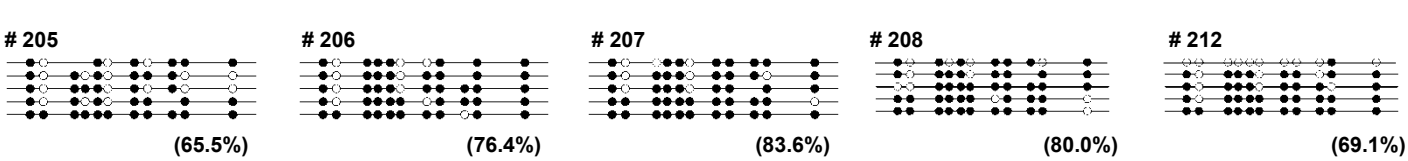

SHS + 4[m] Rec. — MI = 73.1 ± 2.0

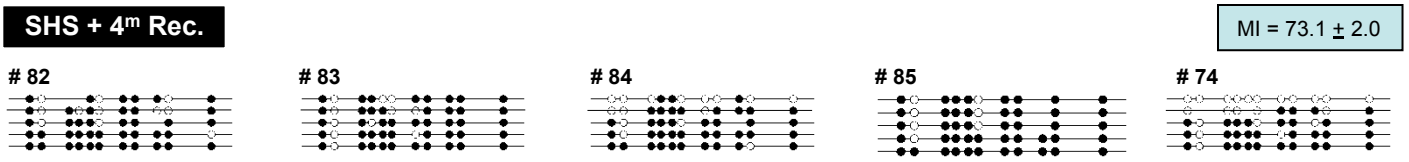

SHS + 7[m] Rec. — MI = 79.6 ± 1.9

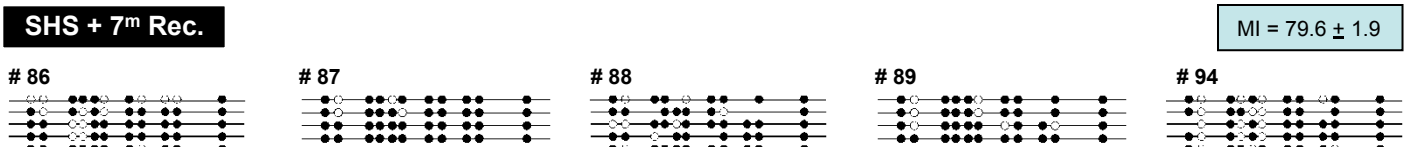

SHS + 10[m] Rec. — MI = 72.4 ± 0.2

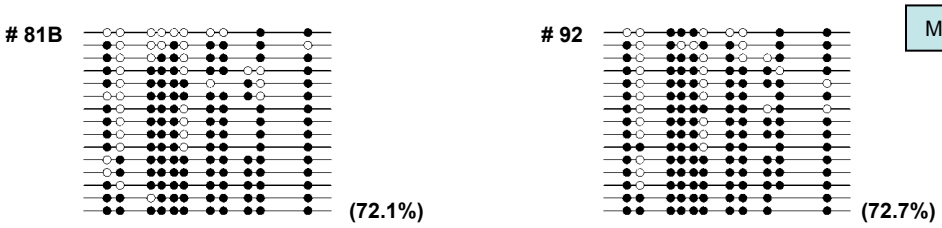

Fig. S4

SINE B1

Control [1] — MI = 60.6 ± 1.7

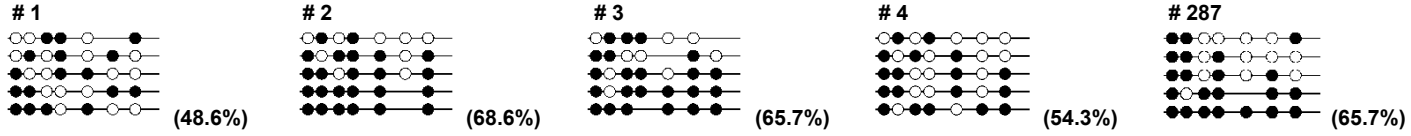

SHS — MI = 57.1 ± 2.4

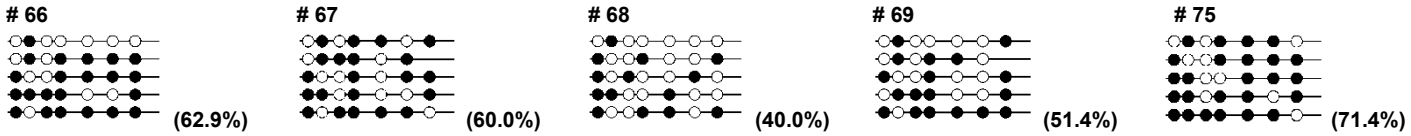

SHS + 1[m] Rec. — MI = 60.0 ± 2.4

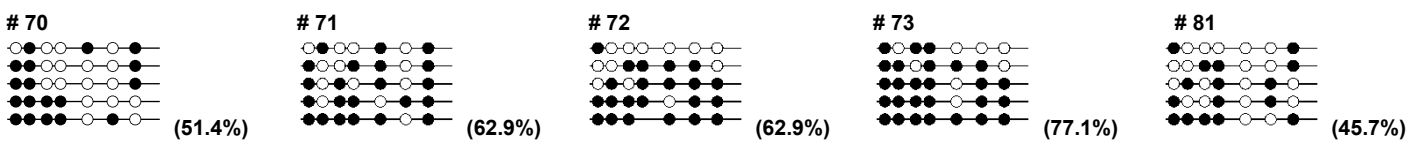

Control [2] — MI = 62.9 ± 1.9

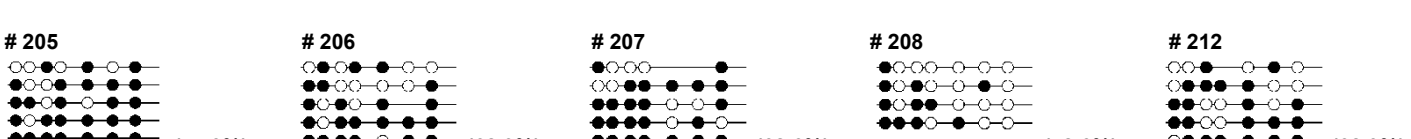

SHS + 4[m] Rec. — MI = 58.3 ± 1.5

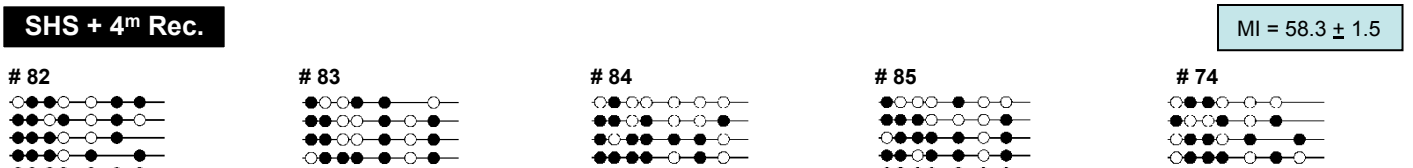

SHS + 7[m] Rec. — MI = 55.4 ± 1.0

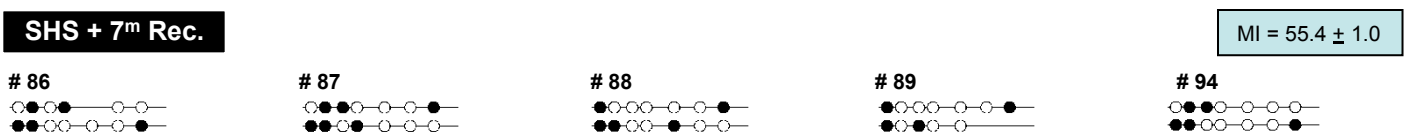

SHS + 10[m] Rec. — MI = 57.6 ± 0.3

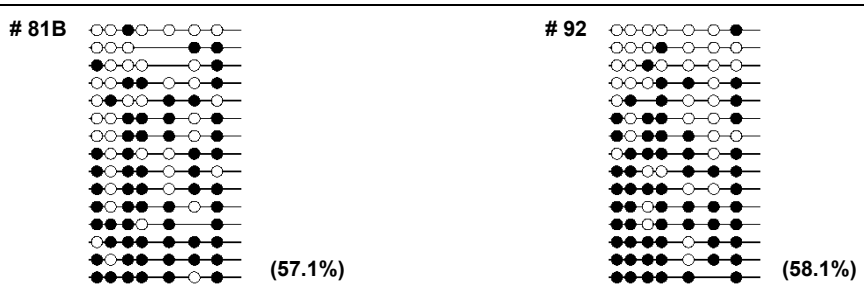

Fig. S5